JVC

Journal of Vibration and Control
17(2) 183–195

DOI: 10.1177/1077546309351222
jvc.sagepub.com
SAGE

Identification of Dynamic Vehicular Axle Loads: Demonstration by a Field Study

L Deng and C S Cai

Abstract

A new identification methodology for dynamic axle loads using the superposition principle and influence surface concept was proposed in the companion paper, in which the effects of various factors such as bridge inertia force, measurement station, vehicle speed, traveling route, number of vehicles, road surface condition, and noise level were investigated through numerical simulations. In this study the proposed methodology is applied to identify the axle loads of a test truck traveling across an existing bridge. The axle load time-histories are obtained and compared to the static axle loads of the test truck. The results show that the identified dynamic axle loads are fluctuating around their static counterparts. The dynamic impact factor and load amplification factor for the axle loads under different vehicle speeds and road surface conditions are also studied. Being able to identify the real dynamic axle loads, the methodology can be applied to improve the current bridge-weigh-in-motion techniques that usually require a smooth road surface and slow vehicle movement to minimize the dynamic effects. The developed methodology will also be useful in identifying real dynamic vehicle forces on bridges, which will provide more reliable live load information for site-specific bridge fatigue assessment and performance evaluation.

Keywords

Acceleration, bridge, deflection, influence surface, strain, superposition principle, vehicle

Received 10 November 2008; accepted 16 September 2009

1. Introduction

Site-specific dynamic axle load information is very useful for bridge designers and researchers in designing new bridges, assessing the condition of old bridges, and maintaining existing bridges. In recent years, many techniques of identifying moving loads on bridges have been proposed, such as the Interpretive Method I (O'Connor and Chan, 1988), the Time Domain Method (Law et al., 1997), the Frequency-Time Domain Method (Law et al., 1999), and the Interpretative Method II (Chan et al., 1999). Laboratory studies (O'Connor and Chan, 1988; Zhu and Law, 2003; Pinkaew and Asnachinda, 2007) as well as field testing (Chan et al., 2000) have also been carried out to verify the proposed methods. A comprehensive literature review of recent research on the identification of moving loads was reported by Yu and Chan (2007).

The dynamic effect of a moving vehicle on a bridge is generally incorporated as a dynamic load allowance (or dynamic impact factor) in many design codes. In the past decades significant amount of analytical investigations on the dynamic vehicle loads have been conducted (Wang and Huang, 1992; Chang and Lee, 1994; Yang et al., 1995; Liu et al., 2002). Field testing has also been carried out to verify the impact factors specified in the design codes (O'Connor and Pritchard, 1985; Park et al., 2005; Shi, 2006) and many researchers showed that the calculated impact factors from field measurements could be higher than the values specified in design codes (Billing, 1984; O'Connor and Pritchard, 1985; Shi, 2006) if the bridge road surface conditions are rough.

To identify site-specific dynamic axle loads that reflect site-specific information such as road surface conditions, a new method of identifying dynamic axle loads using the superposition principle and influence surface concept was proposed in the companion paper (Deng and Cai 2010a). In the present study the proposed method is applied to

Department of Civil and Environmental Engineering, Louisiana State University, Baton Rouge, LA, 70803, USA

Corresponding Author:
C S Cai, Department of Civil and Environmental Engineering, Louisiana State University, Baton Rouge, LA, 70803, USA
Email: cscai@lsu.edu

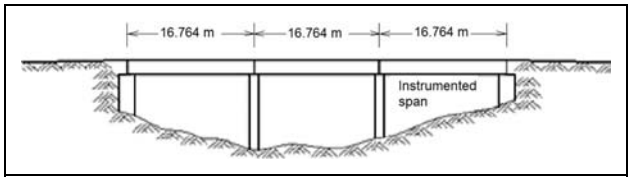

Figure 1. Profile of the test bridge.

identify the axle loads of a truck on an existing bridge. The tested existing bridge is modeled using a three-dimensional finite element (FE) model with the ANSYS program. A full-scale two-axle vehicle model is used to simulate the test truck. The axle-load time-histories are obtained using the methodology developed in the companion paper and are compared with the static axle loads. The results show that the identified dynamic loads are fluctuating around their static counterparts, which demonstrates qualitatively the rationality of the proposed method. The dynamic impact factor and load amplification factor for axle loads under different vehicle speeds and road surface conditions are also discussed by using the identified axle loads.

2. Bridge Testing

2.1. Tested Bridge

The tested bridge is a two-way bridge located over Cypress Bayou in District 61, on LA 408 East, Louisiana. The bridge consists of two separated structures, which are identical and symmetric about the center line of the bridge. Each structure provides a path for traffic in each direction. Since they are separated, only one structure is investigated in this paper.

The bridge structure considered in the present study has three straight simple spans, each measuring 16.764 m (55 ft) in length with zero skew angles (Figure 1). As shown in Figure 2, seven AASHTO Type II prestressed concrete girders with spacing of 2.13 m (7 ft) from center to center are used for the bridge. All girders are supported by rubber bearings at both ends. Each span has one intermediate diaphragm (ID) located at the mid-span as well as two more located at each end of the span, all of which are separated from the bridge deck.

The third span of the bridge was instrumented. A total of seven measurement stations (S1, S2, S3, S4, S5, S6, and S7 corresponding to girders G1, G2, G3, G4, G5, G6, and G7) were selected at the bottom of the seven girders. These measurement stations are 0.305 m (1 ft) away from the mid-span of the corresponding girders to avoid stress concentration due to the diaphragms placed at the mid-span of the girders. Strain gauges, accelerometers, and cable extension transducers were placed at each of the seven stations.

Based on the configuration of the bridge, a FE bridge model was created using the ANSYS program (Figure 3). The bridge deck, girders, diaphragms, shoulder, and railing were all modeled using solid elements, which have three translational degrees of freedom (DOFs) for each node. The rubber bearings were modeled using equivalent beam elements with six DOFs (three translational and three rotational) for each node. Rigid connections were assumed between the rubber bearings and supports and also between the girders and diaphragms. Full composite actions were assumed between the girders and bridge deck.

To obtain more accurate influence surfaces for axle load identification, the bridge model was updated by the authors in another study using the field measurements (Deng and Cai, 2010b). Five parameters including the Young's modulus for the bridge deck, the seven girders, and the diaphragms, respectively; the density of the bridge deck; and the equivalent Young's modulus for the rubber bearings were treated as variables. With the best available information the original values were assumed to be 25.12 GPa, 32.03 GPa, 25.12 GPa, 2323kg/m^3, and 200 MPa, respectively. The five parameters were then updated with two different criteria depending on the purpose of model updating. With the purpose of achieving the best agreement possible between the measured natural frequencies and strains on the seven girders and their counterparts predicted by the FE bridge model, the following updated values for the five parameters were obtained: 29.44 GPa, 35.87 GPa, 10.07 GPa, 2693 kg/m^3, and 53.5 MPa. The five parameters were also updated based on the natural frequencies and deflections of the seven girders, and the following updated results were obtained: 24.77 GPa, 27.67 GPa, 10.0 GPa, 2705 kg/m^3, and 33.06 MPa, respectively. The details are not given here but can be referred to Deng and Cai (2010b).

Significant differences can be found between the two sets of updated parameters obtained with different purposes. As discussed by Deng and Cai (2010b), one possible reason for the differences could be that the measured deflections were larger than the true deflections on the seven girders since the deflection gages were set on sand instead of on a solid base. An overestimated deflection makes the updated bridge model more flexible than it really is. However, as will be shown later, the vehicle axle loads can be identified based on either strain or deflection, as long as the corresponding updated model is used in the identification process.

2.2. Test Truck

The truck used in the bridge testing is a dump truck with a single front axle and a two-axle group for the rear (Figure 4). The static loads for the first, second, and third axle of this truck are 80.0 kN, 95.6 kN, and 95.6 kN, respectively. The distance between the front axle and the center of the two rear axles is 6.25 m, and the distance between the two rear axles is 1.2 m.

Chan and O'Conner (1990) conducted a detailed study on the dynamic effect caused by heavy vehicles, and they concluded that the two groups of axles can be replaced by one equivalent axle acting at the center of the two

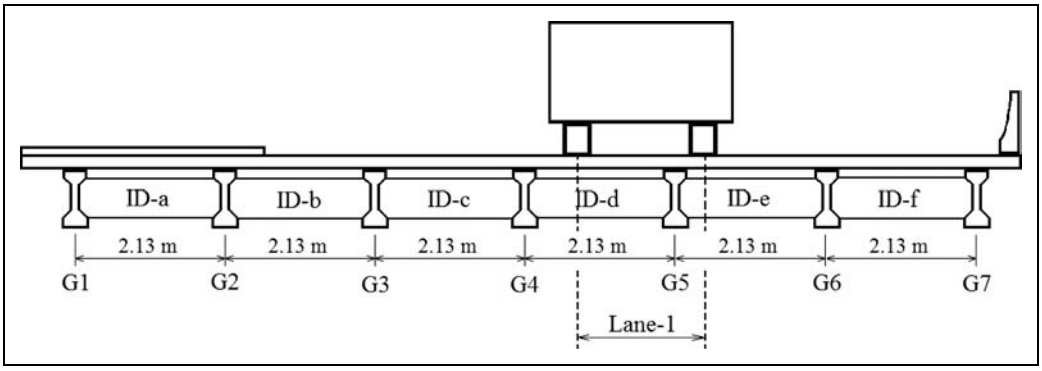

Figure 2. Cross section of the bridge and the position of Lane-1.

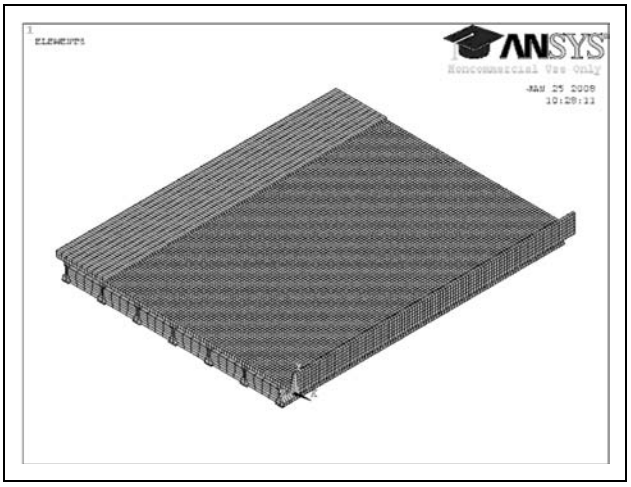

Figure 3. Numerical model of the test bridge.

Figure 4. Dump truck used in bridge testing.

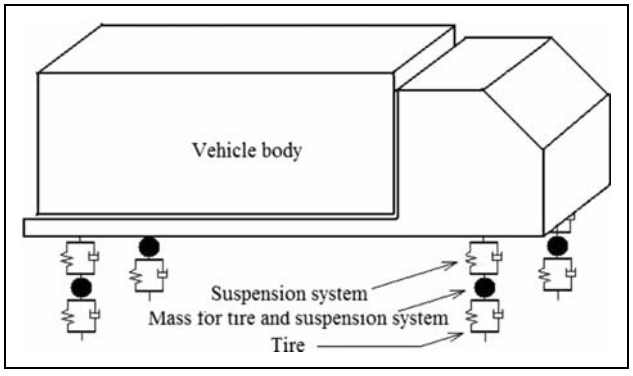

Figure 5. Vehicle model for the dump truck.

groups if the two groups of axles are close enough. To simplify the load identification problem for the three-axle truck, the two groups of rear axles were replaced by one equivalent axle in the present study, and the truck was modeled using a full-scale two-axle vehicle model shown in Figure 5 with eight DOFs (one translational DOF for each of the four wheels as well as the vehicle body in the vertical direction, and three rotational DOFs for the vehicle body). This vehicle model is a combination of a rigid body connected to four masses by a series of springs and damping devices, with the rigid body representing the vehicle body and the linear elastic springs and dashpots representing the tires and suspension systems (Shi, 2006).

2.3. Road Surface Profile

The irregularity (roughness) of the bridge deck was measured by using a laser profiler, which obtains the longitudinal road surface profile along each wheel track. For the purpose of simplicity or due to the limitation of the vehicle-bridge model, in most previous studies two-dimensional (2-D) road surface profiles were used (Yang et al., 1995; Au et al., 2001; Shi, 2006) in which the change of road elevation along the lateral direction was not considered. Considering a three-dimensional (3-D) road surface profile would result in different dynamic wheel loads for the two wheels on the same axle. Since the interest of the present study focuses only on the axle loads, a 2-D road surface profile is used in this paper, though a 3-D road surface profile could be considered using the developed vehicle–bridge coupled system.

Figure 6. Changing the road surface condition by using a wooden bump.

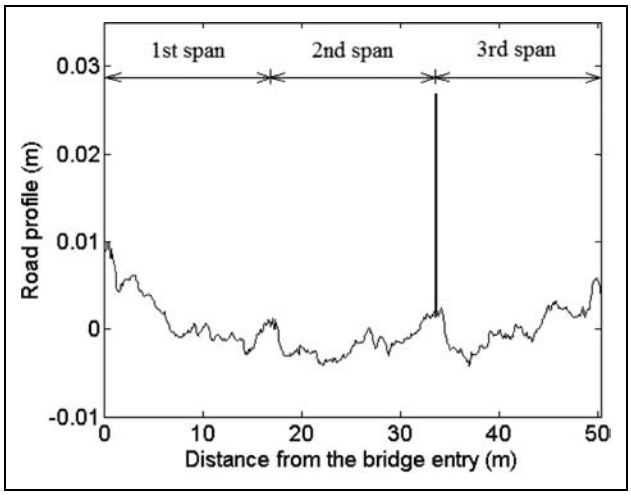

Figure 7. Road surface profile along Lane-1 with the presence of a 0.025 m-high wooden bump.

In order to examine the effect of the road roughness on the accuracy of the identified axle load time history as well as on the the dynamic impact factor, two wooden bumps (named Bump-1 and Bump-2) with equal widths of 0.18 m were prepared. The heights for Bump-1 and Bump-2 are 0.025 m (1 inch) and 0.038 m (1.5 inches), respectively. The two wooden bumps, one at a time, were placed at the entry end of the third span (Figure 6, each span is simply-supported). It should be noted that the main purpose of using wooden bumps in this study is to excite the dynamic effect of the vehicle loads, rather than to represent the real road surface condition, though they can qualitatively reflect the faulting conditions at bridge ends. A faulting of 0.038 m (1.5 inches) is very possible for bridge ends of many existing bridges (White et al., 2005).

Figure 7 shows the measured road surface profile of Lane-1 along the track of the right wheel of the test truck with the presence of Bump-1 (shown as a spike), which changes the original road surface profile by adding a peak at the entry end of the third span (each span is simply supported).

The dynamic effect caused by the measured bridge surface profile without a wooden bump was then examined in a simulation study and compared to the measured

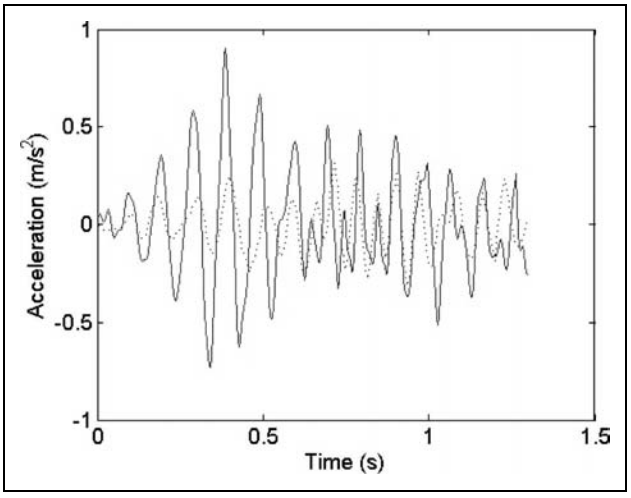

Figure 8. Measured and simulated acceleration from S5 without wooden bump (——, simulated; · · · · · · , measured).

dynamic effect. Figure 8 shows the measured and simulated acceleration from S5 when the test truck is traveling across the bridge at a speed of 17.88 m/s (40 mph). As can be seen from the figure, using the measured road surface profile in the numerical simulation produces larger accelerations than that measured from field testing. One possible reason for this difference could be that the finite element model was updated based on deflections or strains rather than accelerations. Therefore, it is expected that the predicted accelerations are less accurate especially when they are small in cases with good surface conditions because when the responses are small, they are more sensitive to simulation errors. In the vehicle-bridge coupled model the contact between the vehicle tire and bridge was assumed to be a point contact, which may not be able to simulate the real surface contact between the tire and bridge deck well. The use of a two-dimensional road surface profile instead of the real three-dimensional road surface profile in the simulation study could also produce larger dynamic effect than in the real situation (Liu et al., 2002). However, when the road roughness gets worse (by the use of a wooden bump), the results are less sensitive to the assumptions. Figure 9 shows the comparison between the measured and simulated accelerations from S5 with the presence of the two wooden bumps. From the figure, we can see that with the presence of a wooden bump, the predicted bridge accelerations match the measured accelerations well.

3. Axle Load Identification Through Measurements of Field Bridge

Two sets of dynamic test results with vehicle speeds of 13.41 m/s (30 mph) and 17.88 m/s (40 mph), respectively, were processed in which the truck was travelling through the bridge along Lane-1 as shown in Figure 2. For each test

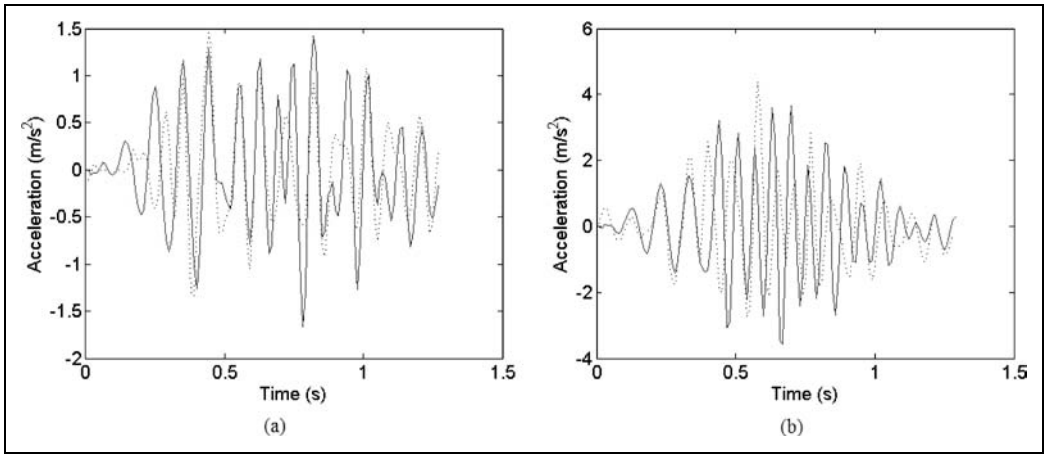

Figure 9. Measured and simulated acceleration from S5 (a) with Bump-1; (b) with Bump-2 present (———, simulated; · · · · · · , measured).

speed the road roughness was changed by placing a wooden bump at the entry end of the span, resulting in three different cases: Case 1, no wooden bump was used; Case 2, Bump-1 was used; Case 3, Bump-2 was used. For each case the bridge dynamic responses from all seven girders, including the strain, deflection, and acceleration, were recorded in time history. Both the deflection and strain time histories were used in the identification process.

The identification of the two axle loads of the test truck is similar to the identification of vehicle loads when two SDOF vehicles are traveling in the same lane one in front the other, as has been studied in the companion paper (Deng and Cai, 2010a). The influence surface for each test, accordingly, was obtained using two unit forces moving side by side along the wheel tracks of the truck to simulate the real axle loads. As has been discussed in the companion paper, identifying two forces at the same time requires bridge responses from at least two measurement stations. In the present study the strain time histories from S4 and S6 and deflection time histories from S4 and S5 were used (the strain time history from S5 was not used because of an obvious problem with the measurement data).

3.1. Axle-load Identification using Deflection Time Histories

The deflection time histories from S4 and S5 and the identified axle loads for the three cases when vehicle speed is 13.41 m/s are shown in Figure 10, in which the three rows I, II, and III represent Case 1, Case 2, and Case 3, respectively. The actual static axle loads, 80 kN for the first axle and 191.2 kN for the second axle, are also marked in the figure.

The figure also shows the deflection caused by the axle loads of the truck, which is calculated by subtracting the deflection caused by the bridge inertia force from the measured deflection. It should be noted that because in reality we cannot measure the bridge acceleration at every point, the simulated acceleration was used in this paper.

The deflection caused by the bridge inertia force can be obtained numerically using the updated model in the following steps. First, the acceleration for each node on the bridge model can be obtained directly after running the program BIRDS-BVI developed in the companion paper; then, the inertia force of each node can be calculated as the product of the mass and acceleration of the node, and the effect of the inertia force of each node on the bridge response can be obtained using the influence surface concept. Finally, the effects of all nodes can be added to obtain the effect of the total bridge inertia force on the response.

From Figure 10 we can easily observe the following: first, in all three cases the deflection caused by the bridge inertia force is less significant than that caused by the vehicle axle loads, especially for the first two cases. Therefore, in this example ignoring the effect of the bridge inertia force may not cause much difference for the identified axle loads. Second, the dynamic effect of the axle loads increases as the road surface condition gets worse (by the use of the wooden bump). The identified axle loads are fluctuating around the static axle loads in all three cases, suggesting that in general the proposed method works well under different road surface conditions. Third, large discrepancies mainly occur at the beginning and the end of the time histories, which was also reported by other researchers (Zhu and Law, 2002; Pinkaew, 2006) and discussed in the companion paper (Deng and Cai, 2010a).

The deflection time histories from S4 and S5 and the identified axle loads for the three cases with the vehicle speed of 17.88 m/s are shown in Figure 11, with similar observations to those of Figure 10. From a comparison between Figure 10 and Figure 11 we can also see that as the vehicle speed increases from 13.41 m/s to 17.88 m/s, the dynamic effect of the axle loads increases, which can be seen from the increase of the maximum dynamic

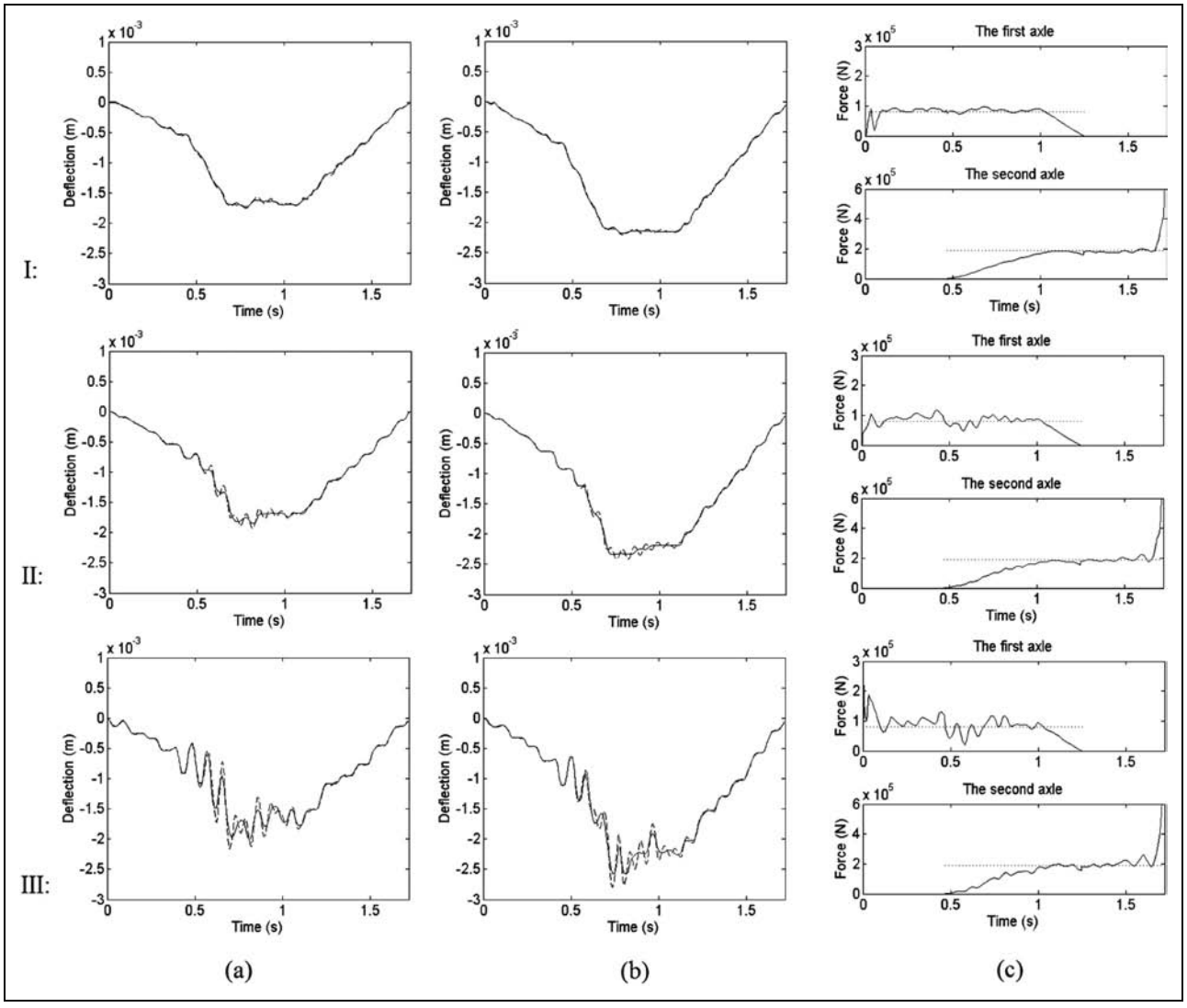

Figure 10. Deflection time histories from S4 (a) and S5 (b) and identified axle loads (c) with (I) no wooden bump, (II) Bump-1, (III) Bump-2 present when the vehicle speed = 13.41 m/s (———, total deflection in (a) and (b) or identified axle loads in (c); – – –, deflection caused by axle loads; · · · · · ·, static axle loads).

deflections from S4 and S5. Results from the two figures also suggest that the vehicle speed does not have a significant effect on the accuracy of the identified results, indicating that the developed methodology can be used under routine traffic conditions. In comparison, most bridge-weigh-in-motion facilities do not work well for normal traveling vehicles and are only reliable for slow traffic (Ansari, 1990; Pinkaew, 2006).

3.2. Axle-load Identification using Strain Time Histories

The strain time histories from S4 and S6 and the identified axle loads for the three cases when the vehicle speed is 13.41 m/s are shown in Figure 12. This figure also shows the strain caused directly by the axle loads of the truck, which is calculated by subtracting the strain caused by the bridge inertia force from the measured total strain.

From the figure it can be seen that: first, in all the three cases the bridge inertia force induced strain is less significant than that caused by the vehicle axle loads. Second, the identified axle loads are fluctuating around the static axle loads in all three cases though the road surface condition is different for each case. Third, large discrepancies mainly occur at the beginning and end of the time histories. These observations are similar to those observed from Figure 10.

The strain time histories from S4 and S6 and the identified axle loads for the three cases when the vehicle speed = 17.88 m/s are shown in Figure 13. Again, similar results to Figure 12 can be observed. These results suggest again that the proposed methodology works well under different road surface conditions and vehicle speeds, which confirms that

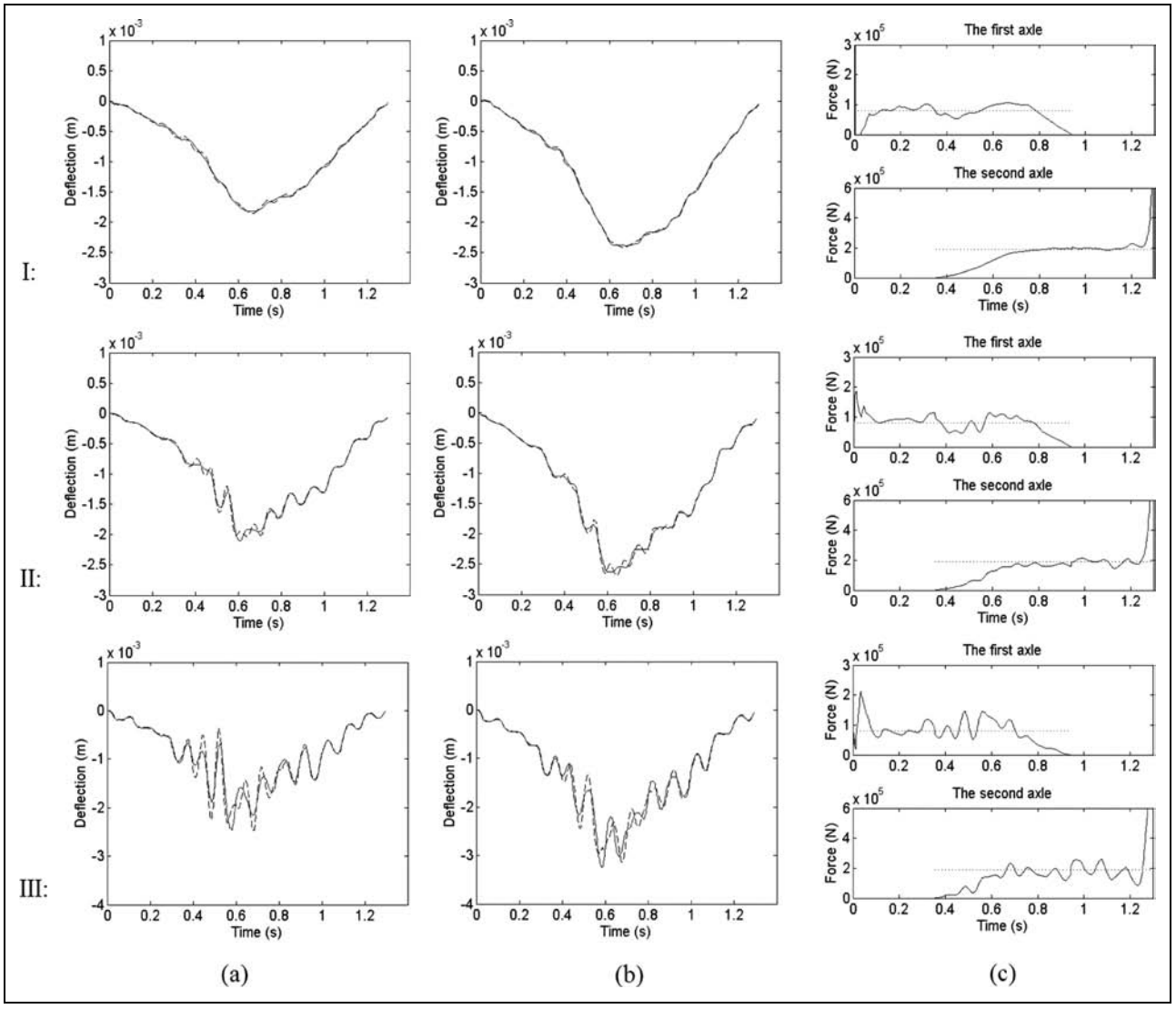

Figure 11. Deflection time histories from S4 (a) and S5 (b) and identified axle loads (c) with (I) no wooden bump, (II) Bump-1, (III) Bump-2 present when the vehicle speed = 17.88 m/s (———, total deflection in (a) and (b) or identified axle loads in (c); – – –, deflection caused by axle loads; · · · · · ·, static axle loads).

the developed methodology can be used for routine traffic conditions.

For the purpose of comparison, a statistic analysis was performed on the time histories of the identified axle loads for all six cases. The mean and standard deviation for both front and rear axles were obtained with the two ends of the time histories being excluded in the analysis. Because generally there is no access to the true dynamic vehicle axle load of field vehicles, the real error of identification is not available. However, the mean value of the partial axle load time-history should be close to the static axle load, though the two values are not necessarily equal to each other. The identified mean values can be used to estimate the truck static weight, while the deviation can be interpreted as the dynamic effects. Results from the statistic analysis are summarized in Table 1, where DIFF is defined as the percentage difference between the mean dynamic axle load and its actual static counterpart. This comparison can also qualitatively verify the developed procedure by observing whether the identified dynamic axle loads are reasonably fluctuating around the static ones.

From the table, the following can be observed. First, the identified results from using deflection and strain are both very good, with the largest difference being under 8% for a single axle and about 3% for the total weight of the truck, which is acceptable in practice, although small discrepancies do exist between the results obtained using the measured deflection and strain time histories, respectively. Second, the identified mean loads are generally greater than the static axle loads for the first axle while less than

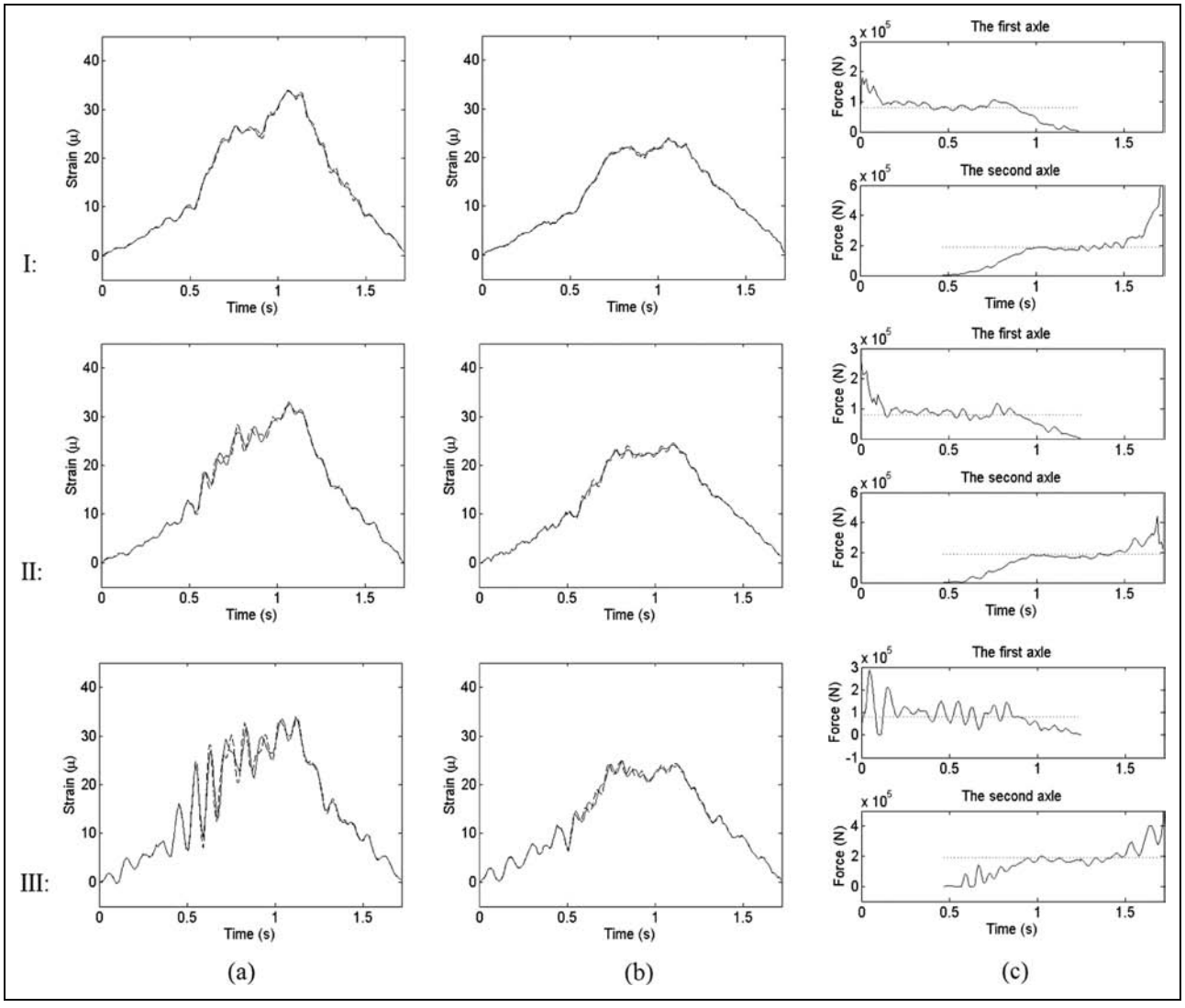

Figure 12. Strain time histories from S4 (a) and S6 (b) and identified axle loads (c) with (I) no wooden bump, (II) Bump-1, (III) Bump-2 present when the vehicle speed = 13.41 m/s (———, total strain in (a) and (b) or identified axle loads in (c); – – –, deflection caused by axle loads; · · · · · ·, static axle loads).

the static axle loads for the second axle. Third, both the vehicle speed and road surface condition have insignificant effects on the identified mean values that approximately correspond to the truck's static weight, indicating that the developed methodology can be used for routine traffic conditions. This would be a significant advantage over most bridge weigh-in-motion systems which usually require smooth road surface conditions and slow vehicle movement to minimize the dynamic effect of vehicle loads (Leming and Stalford, 2002; McNulty and O'Brien, 2003). Lastly, as the road surface condition gets worse the standard deviation of the results gets larger, indicating that the dynamic effect induced by the road roughness becomes more significant.

There are two possible reasons for the difference between the identified static axle loads and the true values. First, the numerical model of the bridge does not represent perfectly the real bridge, which will introduce some error into the prediction of influence surfaces. Second, the speed of the test truck could not be controlled perfectly. For example in this case, it is possible that the truck was driving at a speed faster in the first half than in the second half instead of keeping a constant speed all the way. This is because in the field testing, the room to stop the truck was limited due to a traffic light ahead and the driver tended to slow down in the second half of driving. In this case by assuming a constant speed, a mismatch would occur between the points on the real time history of the bridge response and the corresponding points on the influence surface. As a result, smaller influence surface values would have been used for the first axle, resulting in larger identified loads, while for the second axle larger influence

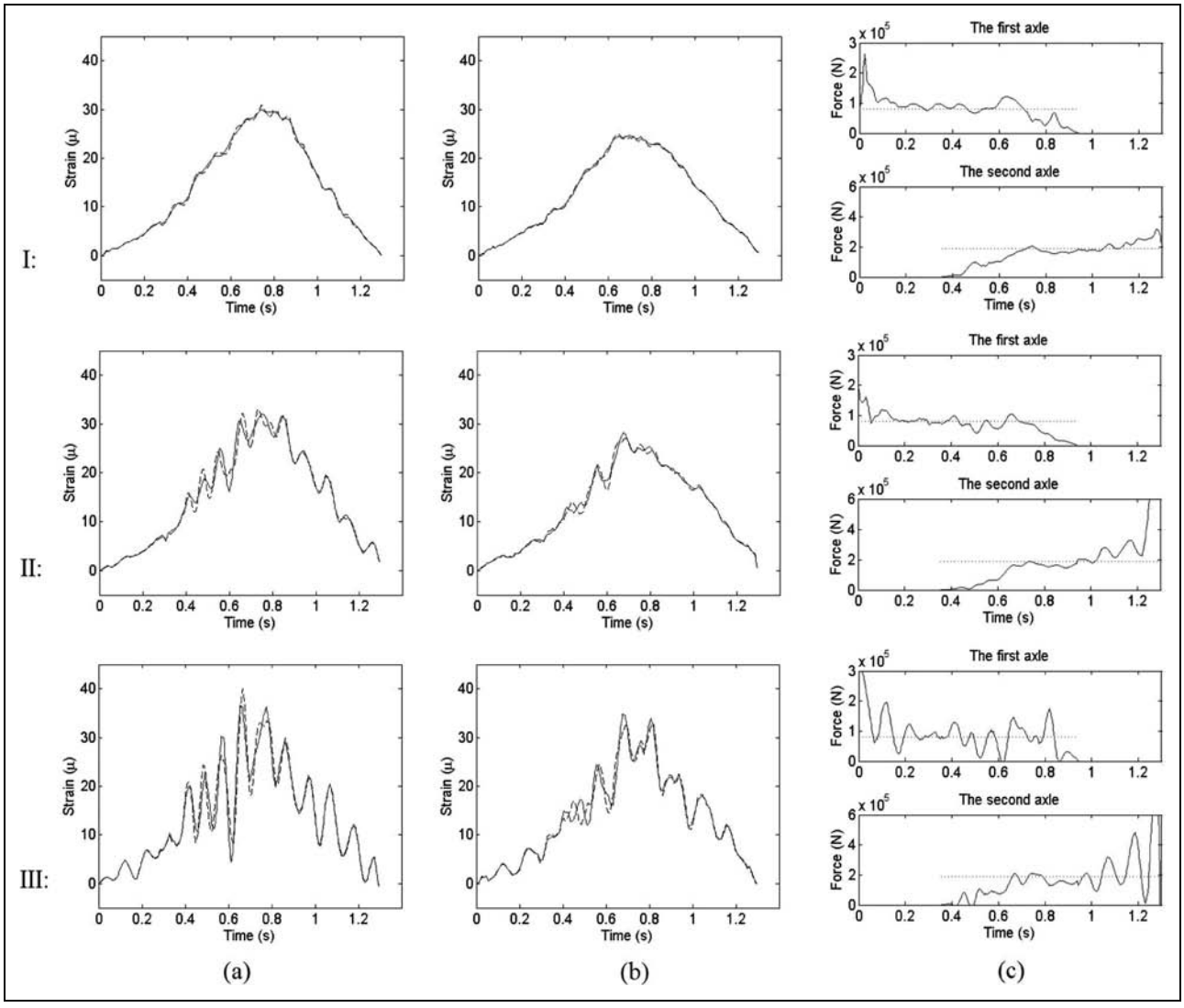

Figure 13. Strain time histories from S4 (a) and S6 (b) and identified axle loads (c) with (I) no wooden bump, (II) Bump-1, (III) Bump-2 present when the vehicle speed = 17.88 m/s (———, total strain in (a) and (b) or identified axle loads in (c); – – –, deflection caused by axle loads; · · · · · ·, static axle loads).

Table 1. Summary of statistic analysis on the identified axle loads

			The first axle			The second axle			Total weight	
Bridge response	Vehicle speed (m/s)	Use of wooden bump	Mean (kN)	DIFF (%)	ST Dev (kN)	Mean (kN)	DIFF (%)	ST Dev (kN)	Mean (kN)	DIFF (%)
Deflection	13.41	No bump	84.14	5.18	7.38	180.60	−5.54	7.15	264.74	−2.38
		Bump-1	85.17	6.46	13.92	182.42	−4.59	11.08	267.59	−1.33
		Bump-2	85.32	6.65	21.37	189.68	−0.79	17.30	275.00	1.40
	17.88	No bump	84.39	5.49	14.23	191.73	0.28	7.95	276.12	1.81
		Bump-1	83.82	4.77	18.71	179.92	−5.90	18.12	263.74	−2.75
		Bump-2	85.12	6.40	23.15	184.68	−3.41	37.73	269.80	−0.52
Strain	13.41	No bump	85.83	7.29	10.14	186.07	−2.68	12.46	271.90	0.26
		Bump-1	85.02	6.27	10.11	181.98	−4.82	14.93	267.00	−1.55
		Bump-2	84.32	5.40	33.66	187.55	−1.91	31.44	271.87	0.25
	17.88	No bump	85.80	7.25	8.81	179.47	−6.13	16.04	265.27	−2.19
		Bump-1	79.22	−0.98	16.28	190.25	−0.50	36.39	269.47	−0.64
		Bump-2	81.90	2.38	31.69	180.55	−5.57	52.15	262.45	−3.23

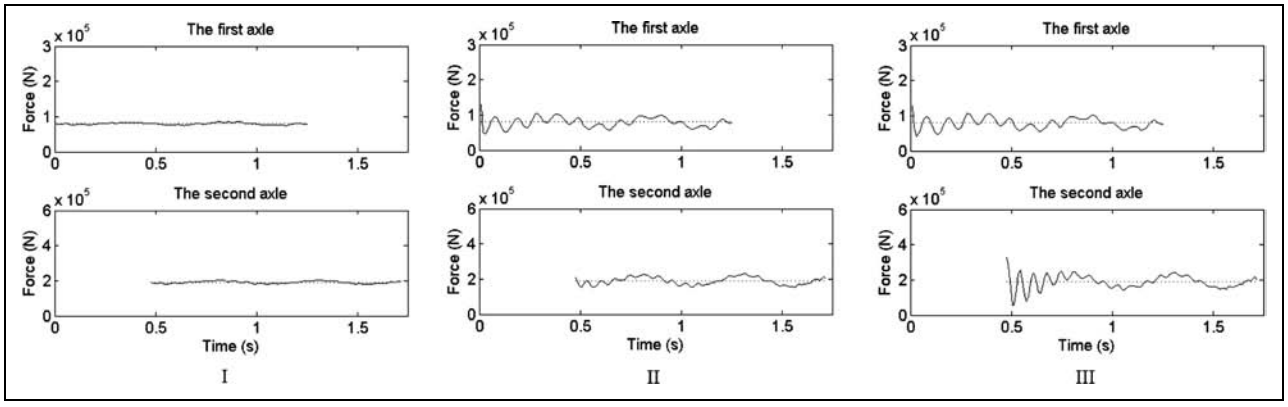

Figure 14. Axle loads obtained from the simulation study with (I) no wooden bump, (II) Bump-1, (III) Bump-2 present when the vehicle speed = 13.41 m/s (———, dynamic axle loads; · · · · · ·, static axle loads).

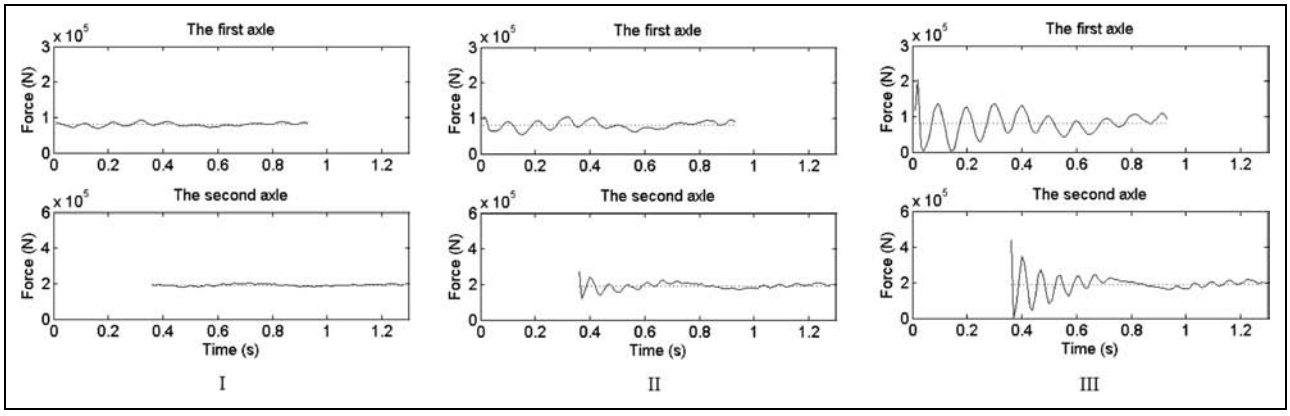

Figure 15. Axle loads obtained from the simulation study with (I) no wooden bump, (II) Bump-1, (III) Bump-2 present when the vehicle speed = 17.88 m/s (———, dynamic axle loads; · · · · · ·, static axle loads).

surface values would have been used, resulting in smaller identified axle loads. Therefore, obtaining the influence surface from field testing and a good control (or knowledge) of the vehicle speed would probably help improve the accuracy of the identified axle loads. Regardless, the accuracy is acceptable for collecting truck load information for bridge design and performance evaluation.

The dynamic interaction forces (i.e. the dynamic axle loads) between the vehicle tires and bridge can also be obtained directly by running the program BIRDS-BVI. For the purpose of comparison, Figures 14 and 15 show the axle loads of the truck obtained from the numerical simulations when the vehicle speed is 13.41 m/s and 17.88 m/s, respectively. As can be seen from both figures, the dynamic effect of the axle loads increases as the road surface condition gets worse (by the use of the wooden bump) and the dynamic axle loads are fluctuating around their static counterparts. Also, as can be seen from the comparison of the two figures, the dynamic effect increases as the vehicle speed increases from 13.41 m/s to 17.88 m/s. All these observations are in good agreement with the identified axle loads.

4. Dynamic Impact Factor and Load Amplification Factor

AASHTO (2004) recommend that in bridge design the static effect of vehicle loads should be increased by an impact factor (also called dynamic allowance factor) to account for the dynamic effect, which can be expressed as:

$$D = (1 + IM) \cdot S \tag{1}$$

where D is the dynamic effect of vehicle loads; $S$is the static effect of vehicle loads; and $IM$is the dynamic allowance factor, which can be calculated as follows:

$$IM = \frac{R_d(x) - R_s(x)}{R_s(x)} \tag{2}$$

where $R_d(x)$ and $R_s(x)$ are the maximum dynamic and static responses of the bridge at location x, respectively.

Using equation (2) and bridge responses under static tests, the impact factors under different dynamic tests are calculated as shown in Table 2. As can be seen from the table, the impact factors calculated from different

Table 2. Impact factor calculated for different load cases.

		Deflection		Strain	
Vehicle speed (m/s)	Use of wooden bump	S4	S5	S4	S6
13.41	No Bump	−0.02	0.01	0.04	0.02
	Bump-1	0.05	0.09	0.03	0.05
	Bump-2	0.12	0.18	0.06	0.09
17.88	No Bump	0.02	0.12	−0.06	0.07
	Bump-1	0.19	0.22	0.00	0.22
	Bump-2	0.39	0.51	0.14	0.51

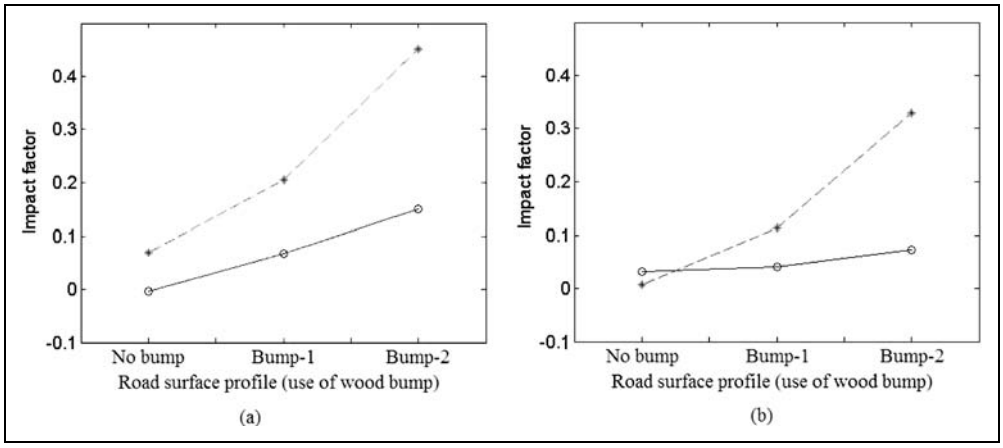

Figure 16. Average impact factor calculated using (a) deflection, (b) strain (o ———, vehicle speed=13.41 m/s; *——, vehicle speed=17.88 m/s).

measurement stations are different, even under the same loading condition.

The effect of road surface condition on the impact factor has been studied by several researchers (Wang and Huang, 1992; Park et al., 2005). Taking an average value for the impact factors from the two measurement stations in Table 2, the impact factors can be plotted against the road surface conditions (in terms of the use of wood bump), as shown in Figure 16.

From the figure, we can clearly see that the vehicle speed has a large impact on the dynamic impact factor. With the speed increasing from 13.41 m/s to 17.88 m/s, the impact factors are more than doubled in most cases. When the vehicle speed is equal to 17.88 m/s, both impact factors obtained from deflection and strain exceed the value of 0.33 specified by AASHTO (2004). The large effect of the vehicle speed on the impact factor was also observed by Au et al. (2001). In their study a sudden increase in the impact factor starts when the speed reaches about 20.83 m/s (75 km/h). It can also be observed from the figure that the road surface condition greatly influences the impact factor, and this impact becomes more significant with the increase in vehicle speed. However, in numerical simulations it should be noted that using a two-dimensional road surface profile would most likely lead to a higher impact factor since the pitch mode of the truck, which causes more dynamic impact, is easier to be excited in this case (Liu et al., 2002).

We also define a dynamic load amplification factor (LAF) as:

$$LAF = \frac{P_{d-\max} - P_s}{P_s} \tag{3}$$

where $P_{d-\max}$is the maximum dynamic load and $P_s$is the static load. From the obtained dynamic axle loads in the previous section, if the two ends of the time histories for the axle loads are ignored we can obtain the maximum dynamic axle loads. The LAFs can then be obtained using equation (3), and the average LAF for the two axles can be plotted against the road surface condition (in terms of the use of the wooden bump) as shown in Figure 17.

Comparing Figures 16 and 17, we can observe a very interesting fact that the calculated load amplification factors are larger than (almost as twice large as) the calculated impact factors. One possible explanation could be that the maximum axle loads and the maximum responses do not occur at the same time. For example, in the present study, the maximum axle loads probably occur immediately after the wheels pass over the wooden bump when a wooden

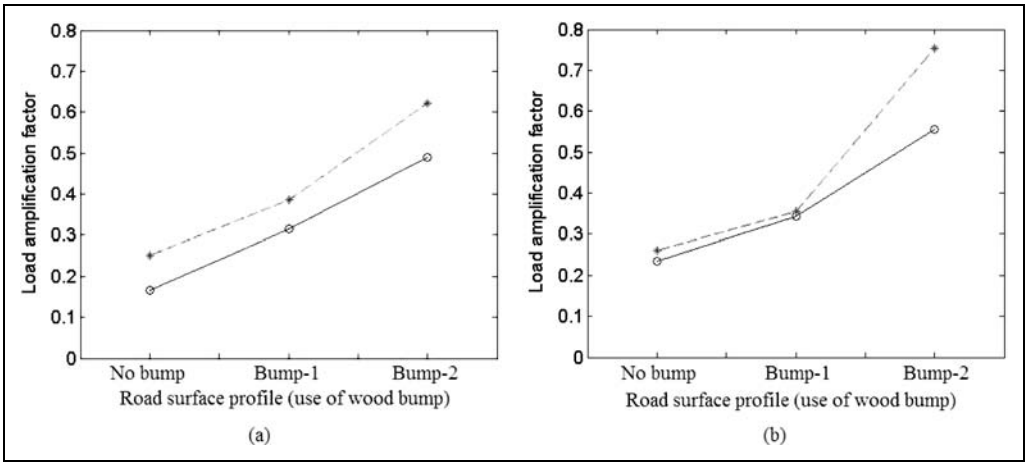

Figure 17. Average load amplification factor calculated using (a) deflection, (b) strain (o ———, vehicle speed=13.41 m/s; *——, vehicle speed=17.88 m/s).

bump is present, as shown in Figures 14 and 15; however, the bridge responses reach a maximum when the rear axle of the truck is approaching the mid-span.

5. Conclusions

A method of identifying dynamic axle loads developed in the companion paper is applied to identify the axle loads of a truck on an existing bridge in Louisiana. Both the deflection and strain time histories are used to identify the truck axle loads. The impact factor and load amplification factor of the axle loads are also examined. Based on the results from the present study, the following conclusions can be drawn:

(1) Both the measured deflection and strain time histories can be successfully used to identify the dynamic axle loads.
(2) The road surface condition and vehicle speed have an insignificant effect on the accuracy of the identified results, which demonstrates the robustness of the proposed methodology under routine traffic conditions.
(3) The calculated load amplification factors are not equal to the impact factors (almost twice the impact factors in this study).
(4) Both the road surface condition and vehicle speed have significant influence on the impact factor. For the examined cases, the impact factor increases as the vehicle speed increases; however, this is not always the case, as demonstrated by many other studies. The impact factor increases significantly as the road surface condition gets worse. It is also interesting to find that the effect of the road surface condition on the impact factor becomes more significant with the increase in vehicle speed.

The demonstrative application of the proposed methodology to identify the real axle loads on a bridge indicates that the proposed methodology can be applied to improve the current bridge weigh-in-motion techniques. The developed methodology will also be useful to predict real vehicle axle forces on bridges, which will provide more reliable live load information for site-specific bridge fatigue assessment and performance evaluation.

Acknowledgement

The authors are thankful to Louisiana State University for providing Economic Development Assistantship to the first writer and Louisiana DOTD and Louisiana Transportation Research Center (LTRC) for making the field test possible. The LaDOTD crew helped conduct the bridge field test. Special thanks go to Mr. Walid Alaywan for coordinating the test and Dr. Doc Zhang for coordinating the surface profiling test. Many graduate students and visiting scholars at LSU also helped prepare and carry out the bridge test.

References

American Association of State Highway and Transportation Officials (AASHTO), 2004, *LRFD bridge design specifications*, Washington, DC.

Ansari, S. A., 1990, "Investigation of improved accuracy limits for dynamic bridge weigh-in-motion system," M.Sc. thesis, Department of Civil Engineering, University of Maryland, College Park, MD.

Au, F. T. K., Wang, J. J., and Cheung, Y. K., 2001, "Impact study of cable-stayed bridge under railway traffic using various models," *Journal of Sound and Vibration* **240(3)**, 447–465.

Billing, J. R., 1984, "Dynamic loading and testing of bridges in Ontario," *Canadian Journal of Civil Engineering* **11**, 833–843.

Chan, T. H. T. and O'Conner, C., 1990, "Vehicle model for highway bridge impact," *Journal of Structural Engineering* **116**, 1772–1793.

Chan, T. H. T., Law, S. S., Yung, T. H., and Yuan, X. R., 1999, "An interpretive method for moving force identification," *Journal of Sound and Vibration* **219(3)**, 503–524.

Chan, T. H. T., Law, S. S., and Yung, T. H., 2000, "Moving force identification using an existing pre-stressed concrete bridge," *Engineering Structure* **22**, 1261–1270.

Chang, D. and Lee, H., 1994, "Impact factors for simple-span highway girder bridges," *Journal of Structural Engineering* **120(3)**, 704–715.

Deng, L. and Cai, C. S., 2010a, "Identification of dynamic vehicular axle loads: theory and simulations," *Journal of Vibration and Control* (in press, doi:10.1177/1077546309351221).

Deng, L. and Cai, C. S., 2010b, "Bridge model updating using response surface method and genetic algorithm," *Journal of Bridge Engineering* (in press, doi:10.1061/(ASCE)BE.1943-5592.0000092).

Law S. S., Chan, T. H. T., and Zeng, Q. H., 1997, "Moving force identification: atime domains method," *Journal of Sound and Vibration* **201(1)**, 1–22.

Law, S. S., Chan, T. H. T., and Zeng, Q. H., 1999, "Moving force identification: a frequency and time domains analysis," *Journal of Dynamic Systems, Measurement, and Control* **12(3)**, 394–401.

Leming, S. K. and Stalford, H. L., 2002, "Bridge weigh-in-motion system development using static truck/bridge model," in *Proceedings of the American Control Conference*, Anchorage, AK, v5, pp. 3672–3677.

Liu, C. H., Huang, D. Z., and Wang, T. L., 2002, "Analytical dynamic impact study based on correlated road roughness," *Computers & Structures* **80**, 1639–1650.

McNulty, P. and O'Brien, E. J., 2003, "Testing of bridge weigh-in-motion system in a sub-arctic climate," *Journal of Testing and Evaluation* **31(6)**, 497–506.

O'Connor, C. and Pritchard, R. W., 1985, "Impact studies on small composite girder bridges," *Journal of Structural Engineering* **111**, 641–653.

O'Connor, C. and Chan, T. H. T., 1988, "Wheel loads from bridge strains: laboratory studies," *Journal of Structural Engineering* **114**, 1724–1740.

Park, Y. S., Shin, D. K., and Chung, T. J., 2005, "Influence of road surface roughness on dynamic impact factor of bridge by full-scale dynamic testing," *Canadian Journal of Civil Engineering* **32(5)**, 825–829.

Pinkaew, T., 2006, "Identification of vehicle axle loads from bridge responses using updated static component techniques," *Engineering Structures* **28**, 1599–1608.

Pinkaew, T. and Asnachinda, P., 2007, "Experimental study on the identification of dynamic axle loads of moving vehicles from the bending moments of bridges," *Engineering Structures* **29**, 2282–2293.

Shi, X. M., 2006, "Structural performance of approach slab and its effect on vehicle induced bridge dynamic response," Ph.D. Dissertation, Louisiana State University, Baton Rouge, LA.

Wang, T. L. and Huang, D. Z., 1992, "Cable-stayed bridge vibration due to road surface roughness," *Journal of Structural Engineering* **118(5)**, 1354–1374.

White, D., Sritharan, S., Suleiman, M., Mekkawy, M., and Chetlur, S., 2005, "Identification of the best practices for design, construction, and repair of bridge approaches," Rep. No. *CTRE Project 02-118*, Iowa Department of Transportation, Ames, IA.

Yang, Y. B., Liao, S. S., and Lin, B. H., 1995, "Impact formulas for vehicles moving over simple and continuous beams," *Journal of Structural Engineering* **121(11)**, 1644–1650.

Yu, L. and Chan, T. H. T., 2007, "Recent research on identification of moving loads on bridges," *Journal of Sound and Vibration* **305**, 3–21.

Zhu, X. Q. and Law, S. S., 2002, "Moving loads identification through regularization," *Journal of Engineering Mechanics* **128(9)**, 989–1000.

Zhu, X. Q. and Law, S.S., 2003, "Dynamic axle and wheel loads identification: laboratory studies," *Journal of Sound and Vibration* **268**, 855–879.